Nanocatalyst-Based Assay Using DNA-Conjugated Au Nanoparticles for Electrochemical DNA Detection

ARTICLE *in* LANGMUIR · OCTOBER 2008

Impact Factor: 4.46 · DOI: 10.1021/la801828a · Source: PubMed

Langmuir

Article

Nanocatalyst-Based Assay Using DNA-Conjugated Au Nanoparticles for Electrochemical DNA Detection

Thangavelu Selvaraju, Jagotamoy Das, Kyungmin Jo, Kiyeon Kwon, Chan-Hwa Huh, Tae Kyu Kim, and Haesik Yang

Langmuir, **2008**, 24 (17), 9883-9888 • DOI: 10.1021/la801828a • Publication Date (Web): 09 August 2008

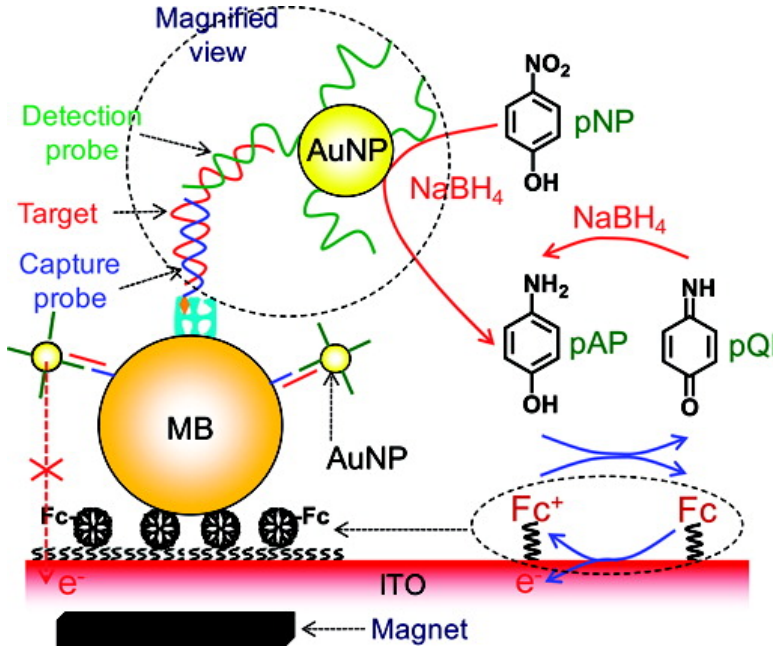

More About This Article

Additional resources and features associated with this article are available within the HTML version:

- Supporting Information
- Access to high resolution figures
- Links to articles and content related to this article
- Copyright permission to reproduce figures and/or text from this article

View the Full Text HTML

Nanocatalyst-Based Assay Using DNA-Conjugated Au Nanoparticles for Electrochemical DNA Detection

Thangavelu Selvaraju, Jagotamoy Das, Kyungmin Jo, Kiyeon Kwon, Chan-Hwa Huh, Tae Kyu Kim, and Haesik Yang*

Department of Chemistry and Chemistry Institute for Functional Materials, Pusan National University, Busan 609-735, Korea

Received June 11, 2008. Revised Manuscript Received July 10, 2008

Compared to enzymes, Au nanocatalysts show better long-term stability and are more easily prepared. Au nanoparticles (AuNPs) are used as catalytic labels to achieve ultrasensitive DNA detection via fast catalytic reactions. In addition, magnetic beads (MBs) are employed to permit low nonspecific binding of DNA-conjugated AuNPs and to minimize the electrocatalytic current of AuNPs as well as to take advantage of easy magnetic separation. In a sandwich-type electrochemical sensor, capture-probe-conjugated MBs and an indium−tin oxide electrode modified with a partially ferrocene-modified dendrimer act as the target-binding surface and the signal-generating surface, respectively. A thiolated detection-probe-conjugated AuNP exhibits a high level of unblocked active sites and permits the easy access of *p*-nitrophenol and $NaBH_4$ to these sites. Electroactive *p*-aminophenol is generated at these sites and is then electrooxidized to *p*-quinoneimine at the electrode. The *p*-aminophenol redox cycling by $NaBH_4$ offers large signal amplification. The nonspecific binding of detection-probe-conjugated AuNPs is lowered by washing DNA-linked MB−AuNP assemblies with a formamide-containing solution, and the electrocatalytic oxidation of $NaBH_4$ by AuNPs is minimized because long-range electron transfer between the electrode and the AuNPs bound to MBs is not feasible. The high signal amplification and low background current enable the detection of 1 fM target DNA.

Introduction

Enzymes (specific biochemical catalysts) have been widely used as signal-amplifying labels in bioassays and biosensors because of their very fast and highly selective catalytic reactions,[1,2] which enable high signal amplification in the presence of bound target biomolecules but no signal amplification in the absence of such molecules. Nevertheless, poor long-term stability of enzymes and their complex preparation and purification procedures necessitate more robust and readily obtainable catalysts.

In recent years, a wide variety of nanocatalysts (nanoparticle-based catalysts) have been developed for catalytic organic synthesis and electrocatalysis.[3,4] Generally, catalytic chemical reactions are much slower than enzymatic reactions, especially in aqueous solutions containing electrolytes. Very importantly, nanocatalysts have many active sites on their surfaces, whereas enzymes have only a small number of active sites, usually just one. Thus, when nanocatalysts are used as labels, signal generation at many active sites per label may allow higher amplification. Moreover, nanocatalysts exhibit good long-term stability, and the preparation of monodisperse nanocatalysts of defined size is readily achieved.[5−7]

To date, there have been but a few examples of catalytic reactions in which nanocatalysts were used as labels.[8−17] For example, catalytic Ag enlargement on Au nanoparticles (AuNPs) (i.e., Ag enhancement) has been extensively adapted in bioassays and biosensors.[8,9] However, special care in the control of deposition time and temperature is required to achieve reproducible assay results.[18] We recently showed that the catalytic reduction of *p*-nitrophenol (pNP) by AuNPs in the presence of $NaBH_4$ can be used for ultrasensitive detection of proteins.[15,16] The reaction is very fast and irreversible but very slow in the absence of AuNPs. Importantly, the reaction product, *p*-aminophenol (pAP), is electroactive within normal potential windows, whereas pNP is not, a feature that enabled us to achieve a high signal-to-background ratio.

Unlike optically active nanoparticle labels, nanocatalyst labels require easy access of small substrate molecules or ions to the nanocatalyst surface even after conjugation between nanocatalyst and biomolecule is formed. If all active sites are covered with biomolecules, the catalytic reaction is significantly hindered. In our previous study, many pinholes remained on AuNPs after adsorption of antibodies, which allowed easy access of pNP.[15] With DNA, single-stranded DNA can bind nonspecifically to AuNPs despite their negative charge,[19,20] but nonspecifically

* E-mail: hyang@pusan.ac.kr. Tel: 82-51-510-3681. Fax: 82-51-516-7421

(1) Hempen, C.; Karst, U. *Anal. Bioanal. Chem.* **2006**, *384*, 572–583.
(2) Porstmann, T.; Kiessig, S. T. *J. Immunol. Methods* **1992**, *150*, 5–21.
(3) Daniel, M.-C.; Astruc, D. *Chem. Rev.* **2004**, *104*, 293–346.
(4) Astruc, D.; Lu, F.; Aranzaes, J. R. *Angew. Chem., Int. Ed.* **2005**, *44*, 7852–7872.
(5) Narayana, R.; El-Sayed, M. A. *J. Phys. Chem. B* **2005**, *109*, 12663–12676.
(6) Rosi, N. L.; Mirkin, C. A. *Chem. Rev.* **2005**, *105*, 1547–1662.
(7) Katz, E.; Willner, I.; Wang, J. *Electroanalysis* **2004**, *16*, 19–44.
(8) Taton, T. A.; Mirkin, C. A.; Letsinger, R. L. *Science* **2000**, *289*, 1757–1760.
(9) Wang, J.; Polsky, R.; Xu, D. *Langmuir* **2001**, *17*, 5739–5741.
(10) Wei, H.; Wang, E. *Anal. Chem.* **2008**, *80*, 2250–2254.
(11) Duan, C.; Cui, H.; Zhang, Z.; Liu, B.; Guo, J.; Wang, W. *J. Phys. Chem. C* **2007**, *111*, 4561–4566.
(12) Gill, R.; Polsky, R.; Willner, I. *Small* **2006**, *2*, 1037–1041.
(13) Zhang, Z.-F.; Cui, H.; Lai, C.-Z.; Liu, L.-J. *Anal. Chem.* **2005**, *77*, 3324–3329.
(14) Cui, H.; Zhang, Z.-F.; Shi, M.-J.; Xu, Y.; Wu, Y.-L. *Anal. Chem.* **2005**, *77*, 6402–6406.
(15) Das, J.; Aziz, M. A.; Yang, H. *J. Am. Chem. Soc.* **2006**, *128*, 16022–16023.
(16) Selvaraju, T.; Das, J.; Han, S. W.; Yang, H. *Biosens. Bioelectron.* **2008**, *23*, 932–938.
(17) Rochelet-Dequaire, M.; Limoges, B.; Brossier, P. *Analyst* **2006**, *131*, 923–929.
(18) Lee, T. M.-H.; Cai, H.; Hsing, I.-M. *Analyst* **2005**, *130*, 364–369.
(19) Cárdenas, M.; Barauskas, J.; Schillén, K.; Brennan, J. L.; Brust, M.; Nylander, T. *Langmuir* **2006**, *22*, 3294–3299.
(20) Sandström, P.; Boncheva, M.; Åkerman, B. *Langmuir* **2003**, *19*, 7537–7543.

10.1021/la801828a CCC: $40.75
Published on Web 08/09/2008

bound single-stranded DNAs are nonhybridizable.[21−23] Thus, the use of thiolated self-assembled monolayers has been preferred for the preparation of AuNP−DNA conjugates.[24−28] When thiolated single-stranded DNAs are conjugated to AuNPs, the thiolated monolayer acts as a physical barrier. In fact, long linear thiolated monolayers are known to significantly limit catalytic reactions on Au surfaces.[29] Nevertheless, Ag enhancement on thiolated DNA-conjugated AuNPs occurs readily,[8,9] indicating that thiolated DNAs do not completely block the Au surface. However, the high negative charge of DNA could hinder the access of negatively charged substrates, which may result in slow catalytic reactions. Tris(2-carboxyethyl)phosphine hydrochloride (TCEP),[30] used to reduce disulfide DNAs, adsorbs strongly onto AuNP.[31] This strong adsorption may also lead to a slow catalytic reaction.

Electrochemical methods have become a promising technique in achieving high sensitivities as well as in realizing portable detection systems.[32−34] Magnetic bead (MB)-based sensors have been widely used because they permit both easy separation and rapid biospecific binding.[35−38] Accordingly, many MB-based electrochemical DNA sensors, especially using AuNP labels, have been developed.[6,39−42] In most cases except the bio-barcode assay, detection limits are much higher than 1 fM.[6,42]

In electrochemical DNA sensors, an electrode typically plays a dual role as a signal-generating surface and a target-binding surface. In MB-based sensors, however, electrodes act only as the signal-generating surfaces, whereas MBs act as the target-binding surfaces.[39] In such sensors, AuNP labels are biospecifically attached to the MBs, not to the electrode. When MBs (attracted by a magnet to an electrode) have a low surface density of the AuNP label, the electron transfer between AuNP and the electrode and between AuNPs becomes difficult.[43,44] Interestingly, in some electrochemical DNA sensors, nanoparticles have been used as electrocatalytic labels.[45,46] When AuNPs are present near an electrode, they can act as an electrocatalytic label as well as a catalytic label. However, if the electrocatalytic reaction by AuNPs is not reproducible, it is difficult to achieve a high signal-to-background ratio (i.e., a low detection limit). In this case, the electrocatalytic reaction should be minimized, and only the catalytic reaction should deliver an electrochemical signal. The use of MBs might be appropriate for meeting this requirement because the long distance between the nanoparticles and electrode could limit the electrocatalytic reaction.

Herein, we describe an Au nanocatalyst-based assay for electrochemical DNA detection that combines the advantages of MBs (coated with streptavidin) and AuNPs (modified with a thiolated DNA monolayer). Capture-probe-conjugated MBs and a ferrocene (Fc)-modified indium−tin oxide (ITO) electrode are used as the target-binding surface and the signal-generating surface, respectively. We first compare the rate of catalytic reduction by AuNPs with that by DNA-conjugated AuNPs. The influences of the thiolated DNA monolayer and TCEP treatment on catalytic reduction are assessed. In addition, we investigate the nonspecific binding of the AuNP−DNA conjugate to the MB−DNA conjugate after formamide treatment. Finally, we examine the dependence of cyclic voltammograms on the concentration of target DNA to determine the detection limit of our DNA sensor.

Experimental Section

Chemicals. Streptavidin-coated MBs (mean diameter = 1.05 μm; product no. 650.01) were obtained from Dynal Biotech (Oslo, Norway). Amine-terminated G4 poly(amidoamine) dendrimer, $NaBH_4$, and pNP were purchased from Aldrich. TCEP, ethylenediaminetetraacetic acid, formamide, tris(hydroxymethyl)aminomethane (Tris), and citrate-stabilized AuNPs [10 nm; 0.01% (w/v) $HAuCl_4$] were purchased from Sigma. The actual size of AuNPs was 8.1 ± 0.8 nm as measured by electron microscopy. All buffer reagents and other inorganic chemicals were obtained from Sigma, Aldrich, or Fluka, unless otherwise stated. All chemicals were used as received, and all aqueous solutions were prepared in deionized distilled water.

The buffer solutions were prepared as follows: The hybridization buffer consisted of 20 mM Tris-HCl, 20 mM ethylenediaminetetraacetic acid, 150 mM NaCl, and 0.05% (v/v) Tween 20 (pH 7.4). The dehybridization buffer consisted of 30 mM Tris, 0.3 M NaCl, and 0.1% sodium dodecyl sulfate (pH 7.4). Phosphate-buffered saline consisted of 0.01 M sodium phosphate, 0.138 M NaCl, and 0.0027 M KCl (pH 7.4). The electrochemical buffer consisted of 50 mM Tris, 10 mM KCl, 0.2 M NaCl, and 7 mM HCl (pH 9.0).

All DNAs were obtained from Genotech (Daejeon, Korea, www.genotech.co.kr). The DNA sequences were originally designed for the detection of the encoding residue 1038 of exon 11 of the *BRCA1* gene.[47] DNAs had the following sequences: biotinylated capture probe, biotin-$(CH_2CH_2O)_3$-5′-AAA GAA GCC AGC TCA A-3′; complementary target DNA, 5′-CTT CAT TAA TAT TGC TTG AGC TGG CTT CTT T-3′; single-base-mismatched DNA, 5′-CTT CAT TAA TAT TGC TTG AGC TGG CTC CTT T-3′; noncomplementary DNA, 5′-CTT CAT TAA TAT TGC TTG AGC GAC TTA AGA T-3′; thiolated detection probe, 5′-GCA ATA TTA ATG AAG-A_{20}-3′-$(CH_2)_3$-SH. The concentrations of DNAs (target, detection probe, and capture probe) refer to those of strands.

Conjugation between AuNPs and Thiolated Detection Probes. AuNPs were conjugated with a 5′-thiol-modified detection probe containing an A_{20} spacer by following a published protocol[48,49] with minimal modification. Briefly, 5 mL of a 4 μM detection-probe

(21) Yang, J.; Lee, J. Y.; Too, H.-P.; Chow, G.-M. *Biophys. Chem.* **2006**, *120*, 87–95.
(22) Yang, J.; Lee, J. Y.; Too, H.-P.; Chow, G.-M.; Gan, L. M. *Chem. Phys.* **2006**, *323*, 304–312.
(23) Lao, R.; Song, S.; Wu, H.; Wang, L.; Zhang, Z.; He, L.; Fan, C. *Anal. Chem.* **2005**, *77*, 6475–6480.
(24) Mirkin, C. A.; Letsinger, R. L.; Mucic, R. C.; Storhoff, J. J. *Nature* **1996**, *382*, 607–609.
(25) Hurst, S. J.; Lytton-Jean, A. K. R.; Mirkin, C. A. *Anal. Chem.* **2006**, *78*, 8313–8318.
(26) Park, S. J.; Taton, T. A.; Mirkin, C. A. *Science* **2002**, *295*, 1503–1506.
(27) Cao, Y. W. C.; Jin, R. C.; Mirkin, C. A. *Science* **2002**, *297*, 1536–1540.
(28) Zhang, J.; Song, S.; Wang, L.; Pan, D.; Fan, C. *Nat. Protoc.* **2007**, *2*, 2888–2895.
(29) Gorman, C. B.; Biebuyck, H. A.; Whitesides, G. M. *Chem. Mater.* **1995**, *7*, 252–254.
(30) Hwang, S.; Kim, E.; Kwak, J. *Anal. Chem.* **2005**, *77*, 579–584.
(31) Lee, C.-Y.; Canavan, H. E.; Gamble, L. J.; Castner, D. G. *Langmuir* **2005**, *21*, 5134–5141.
(32) Katz, E.; Willner, I. *Angew. Chem., Int. Ed.* **2004**, *43*, 6042–6108.
(33) Castañeda, M. T.; Alegret, S.; Merkoçi, A. *Electroanalysis* **2007**, *19*, 743–753.
(34) Merkoçi, A.; Aldavert, M.; Marín, S.; Alegret, S. *Trends Anal. Chem.* **2005**, *24*, 341–349.
(35) Richardson, J.; Hawkins, P.; Luxton, R. *Biosens. Bioelectron.* **2001**, *16*, 989–993.
(36) Matsunaga, T.; Okamura, Y. *Int. J. Nanosci.* **2002**, *1*, 383–389.
(37) Hsing, I.-M.; Xu, Y.; Zhao, W. *Electroanalysis* **2007**, *19*, 755–768.
(38) Zacco, E.; Pividori, M. I.; Alegret, S.; Galve, R.; Marco, M.-P. *Anal. Chem.* **2006**, *78*, 1780–1788.
(39) Paleèek, E.; Fojta, M. *Talanta* **2007**, *74*, 276–290.
(40) Wang, J. In *Electrochemistry of Nucleic Acids and Protein: Towards Electrochemical Sensors for Genomics and Proteomics*; Paleèek, E., Scheller, F., Wang, J., Eds.; Elsevier: Amsterdam, The Netherlands, 2005; pp 369−384.
(41) Kawde, A.-N.; Wang, J. *Electroanalysis* **2004**, *16*, 101–107.
(42) Jaffrezic-Renault, N.; Martelet, C.; Chevolot, Y.; Cloarec, J.-P. *Sensors* **2007**, *7*, 589–614.
(43) Wang, J.; Xu, D.; Kawde, A.-N.; Polsky, R. *Anal. Chem.* **2001**, *73*, 5576–5581.
(44) Ambrosi, A.; Castañeda, M. T.; Killard, A. J.; Smyth, M. R.; Alegret, S.; Merkoçi, A. *Anal. Chem.* **2007**, *79*, 5232–5240.
(45) Polsky, R.; Gill, R.; Kaganovsky, L.; Willner, I. *Anal. Chem.* **2006**, *78*, 2268–2271.
(46) Gao, Z.; Yang, Z. *Anal. Chem.* **2006**, *78*, 1470–1477.
(47) Dunning, A. M.; Chiano, M.; Smith, N. R.; Dearden, J.; Gore, M.; Oakes, S.; Wilson, C.; Stratton, M.; Peto, J.; Easton, D.; Clayton, D.; Ponder, B. A. *Hum. Mol. Genet.* **1997**, *6*, 285–289.

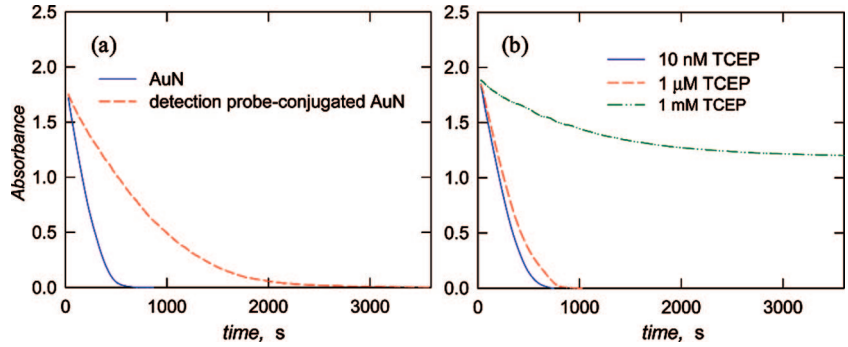

Figure 1. Time course of absorbance at 400 nm for the catalytic reduction of 0.1 mM pNP (a) by bare AuNP or detection-probe-conjugated AuNP in a solution containing 50 mM Tris, 10 mM $NaBH_4$ and 0.18 nM AuNP or detection-probe-conjugated AuNP, and (b) by bare AuNP in a TCEP-containing solution.

solution containing 20 mM TCEP, used for the reduction of disulfide bonds, was mixed with 5 mL of a AuNP suspension (ca. 6 nM). The pH of the mixture was adjusted to pH 7 using 0.1 M NaOH. After incubation for 70 h, detection-probe-conjugated AuNPs were transferred to a 10 mM phosphate buffer (pH 7.4) containing 0.1 M NaCl. After 70 h of aging, the detection-probe-conjugated AuNPs were separated by centrifugation at 20 000*g* for 1.5 h at 4 °C and resuspended in a phosphate-buffered saline. Washing was repeated twice. Finally, the conjugates were dispersed in a 10 mM phosphate buffer (pH 7.4) containing 0.25 M NaCl and 0.02% (w/v) sodium azide in a final volume of 5 mL.

Conjugation between Streptavidin-Coated MBs and Biotinylated Capture Probes. Conjugation between streptavidin-coated MBs and biotinylated capture probes was carried out according to the manufacturer's instructions. Twenty μg of streptavidin-coated MBs was washed with 100 μL of Tris buffer (pH 8.0) with 100 mM Tris, 0.1% (v/v) Tween 20, and 1 M NaCl. Next, streptavidin-coated MBs were suspended in 20 μL of Tris buffer, and 32 μL of 10 μM biotinylated-capture-probe solution was added. The resulting solution was sonicated for 2 min and incubated for 1 h at 20 °C with mechanical shaking. The capture-probe-conjugated MBs were separated using a magnetic separator and washed three times with 100 μL of Tris buffer (pH 8.0) with 250 mM Tris and 0.1% (v/v) Tween 20. The purified conjugates were resuspended in 50 μL of hybridization buffer.

DNA Hybridization and Formation of a DNA-Linked MB−AuNP Assembly. 100 μL of target DNA solution was added to a suspension containing capture-probe-conjugated MBs. The hybridization reaction was carried out for 1 h at 25 °C with mechanical shaking. The hybridized complex was then washed three times with 100 μL of Tris buffer (pH 8.0) containing 250 mM Tris and 0.1% (v/v) Tween 20. The complex was resuspended in 150 μL of phosphate-buffered saline. 40 μL of a suspension of 3 nM detection-probe-conjugated AuNP was added to the resulting solution, which was incubated for 1 h at 25 °C with mechanical shaking. Finally, the target DNA-linked MB−AuNP assembly was formed. The assembly was washed sequentially with 200 μL of phosphate buffer (pH 7.4) containing 100 mM phosphate and 0.1% (w/v) sodium dodecyl sulfate, and then 200 μL of an aqueous solution containing 5% (v/v) formamide, and, finally, twice with 200 μL of phosphate-buffered saline. The formamide was employed to reduce nonspecific binding of DNA.[50] Next, the DNA-linked MB−AuNP assembly was resuspended in 100 μL of electrochemical buffer prior to electrochemical experiments.

Preparation of Working Electrodes and Electrochemical Measurements. The preparation of working electrodes has been previous described.[16] The working electrodes were ITO electrodes modified with partially ferrocene-modified dendrimers (i.e., Fc-D-modified ITO electrodes).

The electrochemical experiments were performed using a CHI708C device (CH instruments, Inc., TX, USA). The electrochemical cell consisted of a working electrode, a Pt-wire counter electrode, and an Ag/AgCl reference electrode. The cell was filled with electrochemical buffer containing 5 mM pNP, 5 mM $NaBH_4$, and a DNA-linked MB−AuNP assembly. $NaBH_4$ was prepared freshly for each experiment. To localize the assembly on the working electrode, a permanent magnet was placed on the bottom of the electrochemical cell. After 15 min of incubation, the signal of the reduced product (pAP) was measured via cyclic voltammetry.

Kinetics of pNP Reduction by AuNP. A standard quartz cuvette with a 1-cm path length was filled with a solution containing 50 mM Tris, 10 mM $NaBH_4$, and 0.18 nM AuNP or detection-probe-conjugated AuNP. After 20 min, a solution containing pNP was added and the suspension was well-mixed. The resulting concentration of pNP was 0.1 mM. The 20-min interval satisfies the induction period for AuNP[51,52] and allowed the solution to reach the reaction temperature of 25 °C. Time-course absorption data were taken at a fixed wavelength of 400 nm. The spectra were recorded with a UV−visible spectrophotometer (Shimadzu UV-1650 PC, Japan). The concentration of AuNPs was estimated by assuming that AuNPs exist as ideal balls tightly packed with Au atoms.[53,54]

Results and Discussion

Influence of Detection Probe and TCEP on the Rate of Catalytic Reduction by AuNP. The thiolated detection probes on the AuNPs might block most of the active sites. As a result, the rate of catalytic reduction of pNP by the conjugated AuNPs might be much less than the rate offered by bare AuNPs. To test this possibility, the kinetics of pNP reduction was studied by measuring the time course of absorbance of pNP solution during catalytic reduction (Figure 1). A high concentration of $NaBH_4$ (10 mM) compared to pNP (0.1 mM) was used to minimize the influence of $NaBH_4$ on reaction kinetics.[55,56] The addition of an AuNPs suspension (or a suspension of detection-probe-conjugated AuNPs) to a solution containing pNP and $NaBH_4$ resulted in fading and ultimate bleaching of the initially yellow-colored solution. Because pNP shows the highest absorption at 400 nm but pAP shows no absorption at this wavelength, spectroscopic measurements were performed at 400 nm. As the amount of AuNPs added to the solution was very small, AuNP absorbance

(48) Lytton-Jean, A. K. R.; Mirkin, C. A. *J. Am. Chem. Soc.* **2005**, *127*, 12754–12755.
(49) Storhoff, J. J.; Elghanian, R.; Mucic, R. C.; Mirkin, C. A.; Letsinger, R. L. *J. Am. Chem. Soc.* **1998**, *120*, 1959–1964.
(50) Hill, H. D.; Mirkin, C. A. *Nat. Protoc.* **2006**, *1*, 324–336.
(51) Pradhan, N.; Pal, A.; Pal, T. *Colloids Surf. A* **2002**, *196*, 247–257.
(52) Mei, Y.; Sharma, G.; Lu, Y.; Ballauff, M.; Drechsler, M.; Irrgang, T.; Kempe, R. *Langmuir* **2005**, *21*, 12229–12234.
(53) Zhang, J.; Song, S.; Zhang, L.; Wang, L.; Wu, H.; Pan, D.; Fan, C. *J. Am. Chem. Soc.* **2006**, *128*, 8575–8580.
(54) Kim, Y.-G.; Garcia-Martinez, J. C.; Crooks, R. M. *Langmuir* **2005**, *21*, 5485–5491.
(55) Panigrahi, S.; Basu, S.; Praharaj, S.; Pande, S.; Jana, S.; Pal, A.; Ghosh, S. K.; Pal, T. *J. Phys. Chem. C* **2007**, *111*, 4596–4605.
(56) Jana, N. R.; Sau, T. K.; Pal, T. *J. Phys. Chem. B* **1999**, *103*, 115–121.

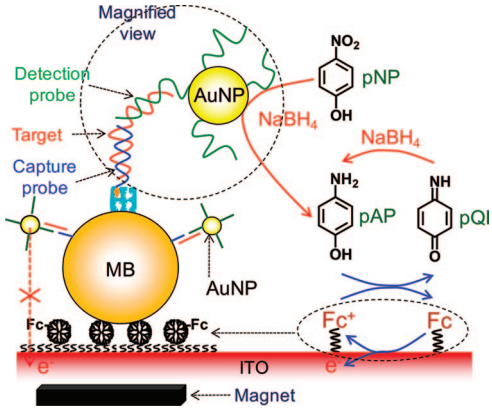

Figure 2. Schematic view of the attraction of DNA-linked MB−AuNP assemblies to an Fc-D-modified ITO electrode and the electrochemical detection of target DNA. MB, AuNP, Fc, Fc-D, ITO, pNP, pAP, and pQI denote magnetic bead, gold nanoparticle, ferrocene, ferrocene-modified dendrimer, indium−tin oxide, *p*-nitrophenol, *p*-aminophenol, and *p*-quinoneimine, respectively.

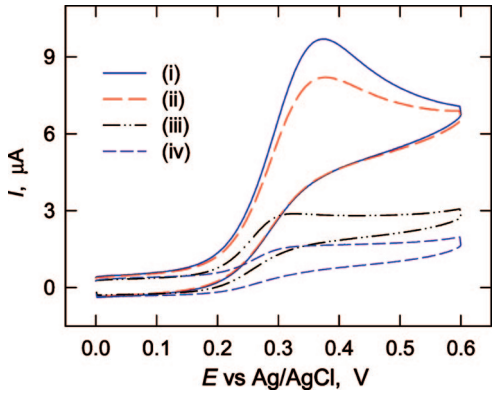

Figure 3. Dependence of cyclic voltammograms on the formamide concentration at a zero concentration of target DNA. DNA-linked MB−AuNP assemblies were washed with solutions of (i) 1%, (ii) 2%, (iii) 4%, and (iv) 5% (all v/v) formamide. Cyclic voltammograms were obtained at Fc-D-modified ITO electrodes to which DNA-linked MB−AuNP assemblies were attracted, after 15 min of incubation in a Tris buffer containing 5 mM pNP and 5 mM $NaBH_4$ at a scan rate of 50 mV/s. In the absence of formamide washing, a very high background current, arising from high nonspecific binding, was observed (data not shown).

barely interferes with the absorption spectrum of pNP. Accordingly, any absorbance change is directly related to a change in the concentration of pNP.[55,56]

The concentration of AuNPs (0.18 nM) in a solution containing bare AuNPs was made the same as that in a solution containing detection-probe-conjugated AuNPs, because the reaction rate depends on the AuNP concentration. The absorbance in a solution containing bare AuNPs decreases more rapidly with time than does that of a solution containing detection-probe-conjugated AuNPs (Figure 1a). This indicates that the catalytic reaction by AuNPs is faster than that by detection-probe-conjugated AuNPs. The time at which the absorbance reaches half of the initial value ($T_{0.5}$) is 177 s in the case of AuNPs but 563 s in the case of detection-probe-conjugated AuNPs. Although the catalytic reaction becomes slower after the modification of AuNPs with the detection probe, the reaction still occurs rather readily. We believe that this is because a high number of unblocked active sites remain on AuNPs even after conjugation, and small pNP molecules can easily access the AuNP surface even through a single-stranded DNA layer.

In this study, TCEP was used to reduce disulfide detection probes prior to the formation of a monolayer of thiolated DNA on AuNPs.[30] Although TCEP, unlike dithiothreitol and other thiol-containing reducing agents, does not contain a thiol group, TCEP also adsorbs strongly onto AuNPs.[31] Moreover, it has been reported that repeated washing could not thoroughly remove TCEP from AuNPs.[31] This strong adsorption might significantly decrease the rate of catalytic reduction. As expected, the catalytic reduction by AuNPs was very slow in a solution containing 1 mM TCEP (Figure 1b). $T_{0.5}$ was much longer than 1 h. However, the rate of catalytic reduction in the presence of 10 nM TCEP ($T_{0.5}$ = 224 s) was similar to that seen in the absence of TCEP ($T_{0.5}$ = 177 s) (Figure 1a). This clearly shows that a low concentration of TCEP does not significantly affect the rate of catalytic reduction. Repeated washing can minimize the adsorption of TCEP onto AuNPs. Therefore, the use of TCEP during conjugation does not cause a significant decrease in the catalytic activity of detection-probe-conjugated AuNPs.

pNP exists in the form of the *p*-nitrophenolate ion at higher pH (pH 9),[55,56] whereas DNA is highly negatively charged. The detection probes on AuNPs might interfere with the approach of negatively charged nitrophenolate and BH_4^- ions to the AuNP surface. This electrostatic repulsion could slow the catalytic reduction. Hence, the reaction in a solution containing detection-probe-conjugated AuNPs was slower than that in a solution containing bare AuNPs but not prohibitively slow. This indicates the easy access of pNP to active sites of AuNPs. Therefore, we could use a detection-probe-conjugated AuNP as an effective catalytic label in this study.

Detection Scheme of the AuNP- and MB-Based Assays. Figure 2 shows a schematic diagram of a sandwich-type electrochemical DNA sensor using AuNPs as catalytic labels. Biotinylated capture probes were biospecifically immobilized onto streptavidin-coated MBs. After target DNAs were hybridized to capture-probe-conjugated MBs, detection-probe-conjugated AuNPs were hybridized. The resulting target DNA-linked MB−AuNP assemblies were attracted to an Fc-D-modified ITO electrode by an external magnet. The MB−AuNP assemblies were incubated for 15 min to generate a large amount of pAP from pNP in the presence of $NaBH_4$. The generated pAP near an Fc-D-modified ITO electrode is electrooxidized to *p*-quinoneimine (pQI) via the electron transfer mediated by Fc. pQI is then reduced back to pAP by $NaBH_4$. Some of the regenerated pAP is reelectrooxidized. As a result, pAP redox cycling by $NaBH_4$ occurs,[15,16] and this considerably increases electrochemical signals. Importantly, pAP is electroactive within normal potential windows, whereas pNP is not;[15,16] this plays a crucial role in achieving a high signal-to-background ratio.

In the detection scheme, MB was used not only for easy separation and rapid biospecific binding but also for low nonspecific binding of DNA-conjugated AuNPs and minimization of the electrocatalytic current by AuNPs. In this MB-based sensor, the electrode acts only as the signal-generating surface, whereas the MB acts as the target-binding surface.[39] If detection probes were immobilized onto an Fc-D-modified ITO electrode, the electrode could have a dual role as a signal-generating surface and a target-binding surface. For this purpose, we also tested a DNA sensor (using only an electrode) that did not use MBs (see the Supporting Information). In this system, we encountered two significant problems: (i) high nonspecific binding of detection-probe-conjugated AuNPs and (ii) high electrocatalytic oxidation of $NaBH_4$ by AuNPs. The AuNP−DNA conjugate showed high nonspecific binding to amine-terminated dendrimers of an Fc-D-modified electrode. Electrocatalytic oxidation of $NaBH_4$ by

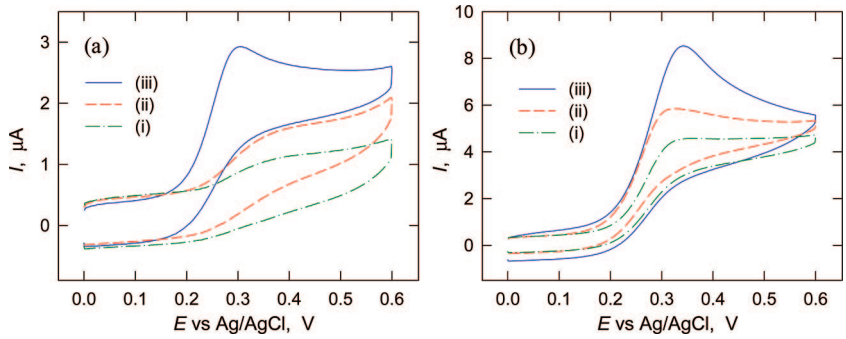

Figure 4. Cyclic voltammograms obtained at Fc-D-modified ITO electrodes to which DNA-linked MB−AuNP assemblies were attracted, after 15 min of incubation in a Tris buffer containing 5 mM pNP and 5 mM $NaBH_4$ at a scan rate of 50 mV/s. (a) Curve i was obtained after only capture-probe-conjugated MB was deposited magnetically, and curves ii and iii were obtained after target DNA-linked AuNP−MB assemblies were deposited magnetically. Target DNA concentrations in curves ii and iii are 0 and 1 fM, respectively. (b) Target DNA concentrations are (i) 10 fM, (ii) 100 fM, and (iii) 1 pM.

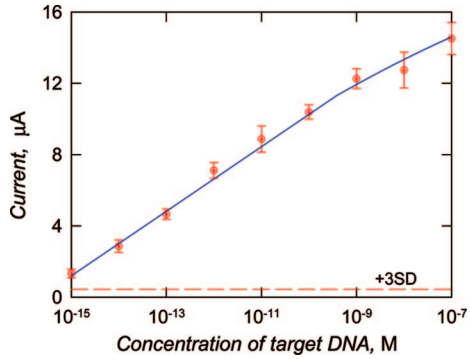

Figure 5. Dependence of the anodic current at 0.35 V in Figure 4 on the concentration of target DNA. All data were subtracted by the mean current at a zero concentration of target DNA. The dashed line corresponds to 3 times the standard deviation (SD) of the current at a zero concentration of target DNA.

AuNPs was very significant because the detection-probe-conjugated AuNPs were close to the ITO electrode. However, the electrocatalytic current was not reproducible. Thus, it was impossible to obtain a high signal-to-noise ratio in the sensor that did not use MBs.

Nonspecific Binding of Detection-Probe-Conjugated AuNPs. Nonspecific binding of DNA-conjugated AuNPs on solid surfaces is more difficult to be lower than that of DNAs because more attractive interactions are caused by the presence of numerous DNA molecules in each nanoparticle.[57] Accordingly, nonspecific binding of detection-probe-conjugated AuNPs to a capture-probe-conjugated MB is considerable. Formamide was reported to effectively reduce nonspecific binding of AuNP−DNA conjugates.[50] Figure 3 shows cyclic voltammograms obtained at a zero concentration of target DNA. Prior to the electrochemical experiment, the MB−AuNP assembly was washed with solutions of 1%, 2%, 4%, or 5% (all v/v) formamide. In the absence of washing, a very high background current, arising from high nonspecific binding, was observed (data not shown). When the percentage of formamide was increased in the washing solution, the nonspecific binding decreased considerably (Figure 3). A solution of 5% (v/v) formamide was therefore used to wash the MB−AuNP assembly in the concentration-dependent experiments described below.

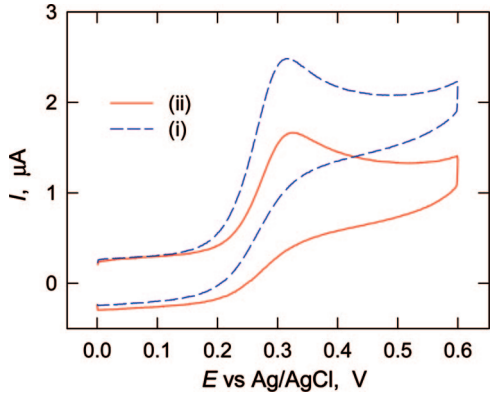

Figure 6. Cyclic voltammograms obtained at Fc-D-modified ITO electrodes to which DNA-linked MB−AuNP assemblies were attracted, after 15 min of incubation in a Tris buffer containing 5 mM pNP and 5 mM $NaBH_4$ at a scan rate of 50 mV/s. The concentration of (i) single-base-mismatched DNA and (ii) noncomplementary was 1 nM. For thermal stringency, the electrodes were washed with a dehybridization buffer for 10 min at 40 °C prior to hybridization of the detection probe.

Concentration Dependence of the Electrochemical DNA Sensor. All curves in Figure 4 except curve i of Figure 4a show cyclic voltammograms obtained after the DNA-linked MB−AuNP assembly was formed in different concentrations of target DNA and was then attracted to Fc-D-modified ITO electrodes. Curve i in Figure 4a was obtained after only capture-probe-conjugated MB was attracted (i.e., without binding of target DNA and detection-probe-conjugated AuNPs to capture-probe-conjugated MBs). Therefore, the cyclic voltammogram of curve i corresponds to the background level of the electrochemical DNA sensor. In our previous study,[16] it was shown that the background level is associated with (i) the capacitive charging current, (ii) the redox current of Fc, (iii) the oxidation current of $NaBH_4$, and (iv) the oxidation current of pAP generated by the catalytic reduction of pNP by an Fc-D-modified ITO electrode. Although multiple processes contribute to the background, the background is sufficiently low to permit low detection limits. It was also shown that MBs had no effect on the catalytic reduction of pNP.[16]

Curve ii in Figure 4a was obtained after the MB−AuNP assembly was formed without target DNA. The difference between the two cyclic voltammograms of curves i and ii corresponds to an increased anodic current of pAP, which results from the nonspecific binding of detection-probe-conjugated AuNP. Curve iii was obtained after the MB−AuNP assembly was formed in the presence of 1 fM target DNA. The peak current of curve iii is much higher than that of curve ii. The current at 0.35 V at a target concentration of 1 fM ($2.7 \pm 0.2\,\mu$A) is clearly higher than that at zero concentration ($1.5 \pm 0.15\,\mu$A), considering that the mean value plus 3 times the standard deviation at a concentration of zero ($2.0\,\mu$A) is lower than $2.7\,\mu$A. Accordingly, the detection limit of this assay was 1 fM. These results indicate that both nonspecific binding and background current are

sufficiently low, and signal amplification sufficiently high, to detect a very low concentration of target DNA.

When AuNPs are near an Fc-D-modified electrode, the electrocatalytic oxidation of $NaBH_4$ by AuNPs occurs. In this MB-based assay, however, the long distance between AuNPs and the electrode minimized this effect. MBs are much larger than AuNPs, and the surface density of detection-probe-conjugated AuNPs on MBs is low (Figure 2).[43] In this case, electron transfer between AuNPs and the electrode, and between AuNPs, does not occur readily.[43,44] It has been reported, however, that direct electron transfer between AuNPs and the electrode is possible when the surface density of AuNPs on MBs is high.[58] Figure 4b shows cyclic voltammograms obtained at higher concentrations of target DNA. As the DNA concentration increases, the peak current increases, but not dramatically. When the cyclic voltammograms of parts a and b of Figure 4 are compared with those in Figure S1b of the Supporting Information, the overall current levels are much less in the former. It seems that the electrocatalytic oxidation of $NaBH_4$ by AuNPs either does not occur or is negligible. The increased current results mainly from electrochemical oxidation of pAP generated by the catalytic reduction by AuNPs.

Figure 5 shows the dependence of the anodic peak current on the concentration of target DNA. The peak current increases almost linearly with increases in the DNA concentration. DNA could be detected over a wide range of concentrations from 1 fM to 0.1 μM (i.e., over 8 orders of magnitude).

To evaluate (i) discrimination of single-base-mismatched DNA and (ii) nonspecific binding of noncomplementary DNA, cyclic voltammograms were obtained when single-base-mismatched DNA or noncomplementary DNA was used in place of target DNA (Figure 6). The current at 0.35 V at a 1 nM concentration of single-base-mismatched DNA ($2.1 \pm 0.2\,\mu$A) was significantly lower than that at a 1 nM concentration of complementary target DNA ($12.2 \pm 0.1\,\mu$A). This result shows that the hybridization of single-base-mismatched DNA with the capture probe is not significant. The current for the noncomplementary DNA ($1.5 \pm 0.3\,\mu$A) was much lower than that for complementary target DNA, indicating that nonspecific binding of noncomplementary DNA is also not significant. These results clearly show that the sensor can discriminate single-base-mismatched DNA and noncomplementary DNA.

Conclusions

We describe a highly sensitive electrochemical DNA sensor that employs AuNPs, MBs, and an Fc-D-modified ITO electrode. AuNPs are used as catalytic labels for signal amplification, MBs are used to achieve low nonspecific binding of DNA-conjugated AuNPs and to minimize the electrocatalytic current by AuNPs, and Fc-D-modified ITO electrodes are employed to obtain a low background current and easy electrooxidation of pAP. The modification of AuNPs with a thiolated DNA monolayer does not significantly decrease the catalytic activity of AuNPs for signal amplification. The pAP redox cycling by $NaBH_4$ provides a high level of signal amplification. The high signal amplification and low background current together allow a very low detection limit of target DNA, 1 fM.

Acknowledgment. This work was supported by the Korea Health Industry Development Institute through Healthcare & Biotechnology Development Program (Grants A050426 and A020605) and the Nano/Bioscience & Technology Program (Grant 2005-01333). This study was financially supported by Pusan National University in the program Post-Doc 2008.

Supporting Information Available: DNA detection at Fc-D-modified ITO electrodes without using MBs. This material is available free of charge via the Internet at http://pubs.acs.org.

LA801828A

(57) Yao, X.; Li, X.; Toledo, F.; Zurita-Lopez, C.; Gutova, M.; Momand, J.; Zhou, F. *Anal. Biochem.* **2006**, *354*, 220–228.

(58) Pumera, M.; Castañeda, M. T.; Pividori, M. I.; Eritja, R.; Merkoçi, A.; Alegret, S. *Langmuir* **2005**, *21*, 9625–9629.